JACS
JOURNAL OF THE AMERICAN CHEMICAL SOCIETY

ARTICLE

pubs.acs.org/JACS

Graphene Actuators: Quantum-Mechanical and Electrostatic Double-Layer Effects

Geoffrey W. Rogers* and Jefferson Z. Liu*

Department of Mechanical and Aerospace Engineering, Monash University, Clayton, VIC 3800, Australia

Supporting Information

ABSTRACT: The electrochemical actuation of covalent carbon materials, such as graphene, immersed in liquid electrolytes has shown immense promise for a myriad of applications. To realize this potential, an intimate understanding of the physics behind the actuation is essential. With the use of ab initio density functional calculations, it is shown that the strain induced in monolayer graphene by the formation of an electrostatic double-layer (DL) is the dominant actuation mechanism. The DL-induced strain (∼1%) is found to exceed the quantum-mechanical strain (∼0.2%) due to charge injection only, for charges and electric potentials of greater than −0.08 e/C-atom and 1 V, respectively. Various methods of calculating the graphene atomic charges based on first principle charge densities are compared and contrasted. The electrochemical charge-strain and potential-strain relationships for monolayer graphene are shown to be parabolic in nature. This study proves that the origin of the high electrochemical strains in covalent carbon materials is the electrostatic DL potential, and demonstrates the true viability of using monolayer graphene for nanoelectromechanical systems (NEMS) actuators.

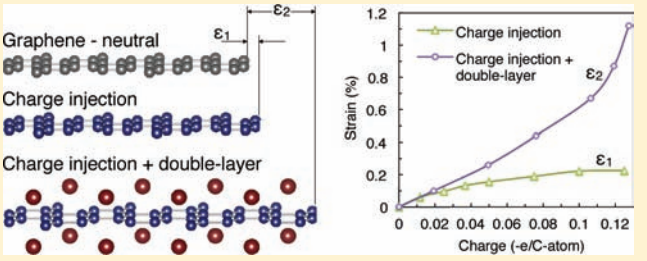

INTRODUCTION

Research into the development of advanced actuation materials has been intense during the past decade, with a diverse range of potential micro/nanoelectromechanical systems (MEMS/NEMS) applications at the ready. One such material developed is that proposed by Baughman et al. in 1999,[1] who synthesized single wall carbon nanotube (SWNT) sheets and demonstrated this material's exceptional electrochemical actuation upon immersion in an aqueous electrolyte. Following this initial demonstration, many studies have sought to refine this novel actuator material via both experimental and theoretical approaches.[2−4] More recently, with its discovery in only 2004,[5] researchers began to investigate graphene as a potential high performance actuator material. Because of its unique electronic properties,[6−8] graphene has attracted a lot of interest with single and multilayer graphene actuators having already been shown.[9−11]

To realize the full potential of these new materials, an in depth understanding of the exact mechanism behind their actuation is vital. In their original manuscript, Baughman et al.[1] postulated that the high SWNT sheet strains measured upon electrolyte immersion and charging were likely due to some combination of two phenomena: quantum-mechanics and the electrostatic double-layer (DL) that forms aside a charged surface. Several groups have sought to investigate the strain due to these two phenomena theoretically, using various approaches including density functional theory (DFT).[12−15] Two of these groups studied the quantum-mechanical actuation of graphene due to simple charge injection using so-called jellium (uniform compensating background charge),[12−14] while the other sought to isolate the two phenomena by simulating the electrostatic DL as a 2D shell of jellium.[15] However, the latter study could not account for the finite size of the ions present in real DLs, and thus could not accurately consider the electrostatic interaction between adjacent ions. An alternative to this DL modeling is the use of Monte Carlo molecular dynamics, which has been used by researchers to investigate electrochemical DL capacitance.[16] However, this treats the DL ions as hard spheres, failing to account for the important motion and interaction of electrons in both the electrode and the DL.[17]

To date, there is yet to be a study incorporating the complete ion−ion, ion−electron, and electron−electron interactions that exist in real electrochemical DLs. Despite concerted efforts by many researchers, there remains a need for a comprehensive understanding of the mechanism behind the electrochemical actuation of covalent carbon materials. Via ab initio density functional methods, this article investigates the physics behind the actuation of monolayer graphene immersed in an ionic liquid (IL) electrolyte. Interest in ILs has been intense in recent times, predominantly due to their high energy storage capacities in electrochemical DL supercapacitors.[18−20] Their solvent-free nature means that IL-based DL devices are not affected by solvent presence, unlike aqueous electrolytes, allowing these devices to reach maximum DL charge concentrations.[19] In addition, ILs show stability across higher electrochemical windows (∼5 V) than aqueous and organic electrolytes.[19,20] As such,

Received: March 1, 2011
Published: June 14, 2011

dx.doi.org/10.1021/ja201887r | J. Am. Chem. Soc. 2011, 133, 10858–10863

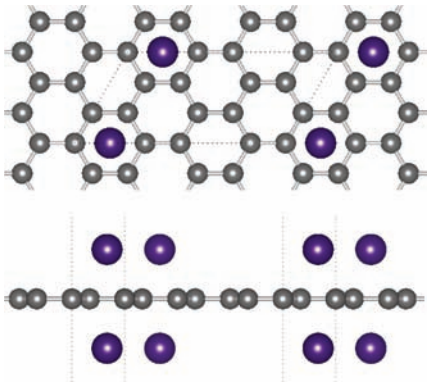

Figure 1. A C_{12} unit cell was used for both the jellium and DL charging of monolayer graphene, with small-silver spheres representing the C-atoms. For DL charging only, DL ions (large-purple spheres) were introduced aside the graphene.

it is both timely and topical to investigate the use of ILs in electrochemical actuators, which this article incorporates. This full ionic and electronic study facilitates the direct probing of the quantum-mechanical and electrostatic DL effects, and their relative contributions to the overall actuation of covalent carbon materials.

COMPUTATIONAL METHOD

DFT calculations were performed using the Vienna ab initio simulation package (VASP v.5.2.2), making use of the projector augmented wave (PAW) pseudopotentials and the generalized gradient approximation (GGA).[21,22] A plane wave cutoff energy of 400 eV was used throughout. Figure 1 shows the C_{12} graphene unit cell used in this study, with two DL ions located on opposing sides of the graphene monolayer over a C-ring center (for atomic coordinates, see Supporting Information, Figure S1 and Table S1). Simulated-annealing molecular dynamic simulations revealed this configuration to be the absolute ground state. Lithium (Li), calcium (Ca), barium (Ba), potassium (K), and sodium (Na) DL ions were tested. The same model as per Figure 1 was used to simulate the charging of graphene in the absence of an electrolyte (jellium simulations), albeit without the DL ions. In all cases, an $18 \times 36 \times 1$ Monkhorst-Pack gamma-centered *k*-point grid was adopted.

To simulate true monolayer graphene using the plane wave code, very high vacuum volumes were included adjacent to the graphene layer to mitigate interlayer electrostatic interactions. Earlier DFT studies employing periodic boundary conditions only separated adjacent graphene layers and individual SWNTs by less than 20 Å.[12−14] Sun et al. showed that there exists a considerable amount of variation in the graphene strains per unit charge injected for varying interlayer spacings of up to 12 Å.[13] Our investigations revealed that it is necessary to separate adjacent layers by at least 60 Å in order to simulate isolated monolayer graphene with jellium charge compensation. This is based on the convergence of the graphene electromechanical strain as a function of the interlayer spacing for a given charge injection (see Supporting Information, Figure S2). Lower values than this are feasible for models incorporating electric DLs, such as that of Pastewka et al.,[15] as the DL screens the interlayer electrostatic interactions. As such, an interlayer spacing of 60 Å was adopted throughout for monolayer graphene, providing a good balance between simulation accuracy and computational effort.

To study the DL charging of a single graphene layer, dopant atoms were introduced aside the graphene in accordance with Figure 1 to simulate the complete immersion of the graphene in a molten salt IL electrolyte. We employed a molten salt electrolyte rather than a room temperature IL (RTIL) in our DFT calculations in order to circumvent the severe computational expense associated with modeling the latter.

Table 1. Comparison between the Computational and Theoretical/Experimental[29] Graphite Intercalation Charge Transfers (e/C-atom)

	Li	Ba	Ca	Cl
Bader	−0.14	−0.15	−0.22	0.06
DDEC	−0.10	−0.05	−0.12	0.05
Hirshfeld-I	−0.02	−0.05	−0.04	0.07
ISA	0.05	−0.25	−0.12	0.05
Theory/experiment	−0.17[30]	−0.19[31]	−0.28[12]	0.03[12]

Further, we simulate ILs rather than aqueous electrolytes due to the applicational benefits discussed earlier, which should give rise to optimal electrochemical actuation performance. Charge injection to the graphene layer was achieved by allowing the electrons to transfer freely between the DL ions and graphene during self-consistent electronic relaxation. This was done for a range of graphene-DL ion separation distances in order to simulate varying DL strengths (see Supporting Information, Figure S3). In all cases, the graphene and DL ions were allowed to move freely parallel to the plane of the graphene, but were locationally fixed along the perpendicular. The VASP source code was modified to achieve this, allowing the cell geometry and ionic positions to completely relax in the plane of the graphene layer only.

Given this method of graphene charge injection, it was necessary to establish a procedure to measure the charge transferred between the graphene layer and the DL ions. There are a vast number of approaches available to do this, with much scrutiny as to their accuracy for various systems. For a summary and analysis of the available methods, see the recent article by Manz and Sholl.[23] On the basis of recent demonstrations and reliability, four methods were tested in the present work to calculate the electronic charge transfer.[24] The first of these is the Bader method, which calculates the charge density zero flux surfaces and uses these to assign the electronic charges to atoms.[25] This so-called basis set method has been widely applied to many systems over time, producing reliable results on most occasions. The second is the density-derived electrostatic and chemical (DDEC) method, which is a more recent self-consistent approach.[23] In the short time since its inception, this method has been proven accurate for many molecules. The third method is the iterative-Hirshfeld (herein denoted Hirshfeld-I) scheme,[26] a self-consistent method based on the traditional Hirshfeld atom.[27] Finally, the iterative stockholder atom (ISA) was tested, which similar to the Hirshfeld-I scheme self-consistently assigns a portion of the grid-based charge density to each atom.[28] In the present work, these four methods were initially tested for some well studied graphite intercalation compounds. For this, an XC_6 unit cell was used, where X represents the intercalant species. The structure was fully relaxed in all directions during the ab initio calculations, with all simulation parameters equivalent to those of the monolayer graphene model specified above, including a similar density *k*-point set of $36 \times 36 \times 36$. As shown in Table 1, the results indicated that the Bader, DDEC, and Hirshfeld-I methods were all in relative agreement, reliably producing the correct direction of charge transfer (graphene charge polarity). The ISA method, on the other hand, failed to predict the correct charge polarity for the case of Li intercalation, which is well understood from theory and experiment to be negative. Accordingly, the Bader, DDEC, and Hirshfeld-I methods were used for subsequent graphene charge transfer calculations.

RESULTS AND DISCUSSION

The charge−strain relationships for monolayer graphene in the presence of a simulated Li ion DL using these charge apportionment methods are shown in Figure 2. As mentioned

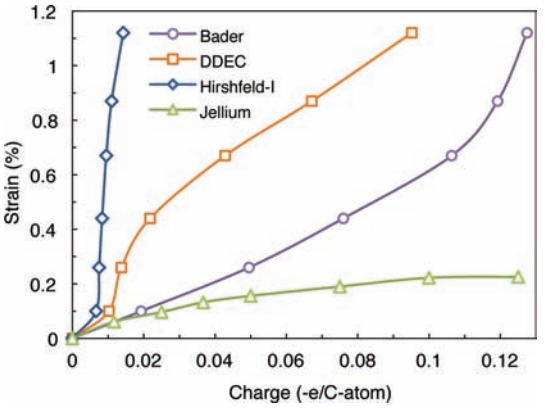

Figure 2. Strain-contribution of the electrostatic DL on monolayer graphene, with charge apportioned via the Bader, DDEC, and Hirshfeld-I methods. Jellium strains are also shown, which accurately represent the quantum-mechanical strain resulting from charge injection only, using large vacuum volumes to simulate isolated monolayer graphene. Lines connect measured data for visualization purposes.

previously, Ca, Ba, K, and Na DL ions were tested along with Li, for which the results were found to be very similar (see Supporting Information, Figure S4). Also shown in Figure 2 is the injection of charge to monolayer graphene in the absence of an electrolyte (jellium simulations). By comparison with earlier computational studies, which predicted graphene strains of 0.3−0.6% for charges of −0.05 e/C-atom,[12−14] the present jellium strain (~0.16%) appears to be significantly less. However, recall that these previous studies used much smaller vacuum volumes, which we found result in artificial graphene strains due to interlayer electrostatic interactions and the self-energy contribution of the jellium. Similar jellium strains to these earlier studies have been predicted using the model herein for interlayer spacings of less than 20 Å (see Supporting Information, Figure S2). As we employ large vacuum volumes adjacent to the graphene layer (60 Å), the present jellium strains more accurately represent true quantum-mechanical actuation resulting from C−C bond expansion due solely to charge injection. In addition to this difference in the magnitude of the predicted strains, the present jellium charge−strain relationship differs from those parabolic dependencies reported previously by some for graphene.[12,14] Through the inclusion of large vacuum layers adjacent to the graphene layer in the present computations, interlayer electrostatic interactions and jellium self-energy effects are mitigated, which we postulate give rise to the artificial parabolic dependencies predicted by others. To reinforce this, Sun et al. present a similar trend to that herein for the jellium charging of graphene, albeit with an interlayer spacing of only 12 Å and higher strain magnitudes.[13]

Comparing the DL and jellium results, it is immediately evident from all charge methods that the electrostatic DL has a significant effect on the graphene strain. Not only does the DL presence induce higher strains for moderate charge injection (0−0.08 electrons per C-atom), but it enables the graphene to generate strains in excess of 1%. According to the jellium data, such high strains are not otherwise possible via the quantum-mechanical effect alone. The significance of this result is that it proves that the electrostatic DL effect is dominant in electrochemical actuators for high charge injection (>−0.08 e/C-atom). While this result is for an IL electrolyte, and thus ultimately represents the optimum DL strain that could be produced by an electrochemical actuator, we expect that the DL contribution to the overall strain will still be significant in the case of an aqueous electrolyte. Pastewka et al. predicted the strain of a SWNT in the presence of an aqueous electrolyte to be double that in a vacuum for charge injections of greater than −0.1 e/C-atom,[15] which points to a significant contribution to the strain by the aqueous DL. To validate our computed strains, we draw comparison to the experimental findings and predictions of Baughman et al.[1] First, via the experimental actuation of aqueous electrolyte filled SWNT sheets, comprising a mechanical entanglement of bundled SWNTs, strains of greater than 0.2% were reported. On the basis of these findings, Baughman et al. proceeded to estimate the actuation performance that could be expected of unbundled SWNTs in an aqueous electrolyte. Via maximization of the gravimetric surface area in this case, they predicted strains on the order of 1% for unbundled SWNTs. In the present study, strains of greater than 1% were observed for monolayer graphene in the presence of an IL electrolyte. This quantitatively agrees with the unbundled SWNT strain prediction by Baughman et al. since the gravimetric surface area of monolayer graphene is optimal (graphene resembles a perfectly 2D structure), and we employ an IL electrolyte, for which maximum DL charge concentrations are attainable.[19]

In terms of the different charge methods, the Bader approach indicates a piecewise-parabolic relationship between the monolayer graphene charge and strain for the Li DL. Similar trends are observed for the other DLs tested (see Supporting Information, Figure S4). For simplicity, we will refer to these trends generally as quasi-parabolic, since they are not parabolic in the traditional sense. These trends agree qualitatively with previous works incorporating localized DLs, including experimental[1] and numerical studies,[15] and can be explained by considering a simplified total energy (E_{tot}) model,[32] where

$$E_{tot} = \frac{1}{2}ks^2 - q\phi + \frac{1}{2C}q^2 \quad (1)$$

Here, k is the elastic constant of graphene, s is the deformation, q is the quantum charge, ϕ is the electrostatic potential, and C is the differential capacitance. The thermal energy has been assumed negligible, and there is no externally applied force and thus no work term. The internal force (F) can be equated to these terms of the energy equation by differentiating it with respect to the deformation (s), giving

$$ks = F + \frac{\alpha}{2}q^2 \quad (2)$$

where α is a simplified capacitive coupling coefficient.[32] Given that at static equilibrium the internal forces (F) reduce to zero, the deformation and thus DL-induced strain becomes a quadratic function of the injected charge: $s \propto q^2$. Interestingly, the DDEC and Hirshfeld-I methods do not produce such a parabolic trend, but still support the fact that the DL significantly contributes to the overall strain. The charge-strain magnitudes given by the DDEC method are in relative agreement with those of the Bader method. The Hirshfeld-I method, on the other hand, estimates the graphene charges to be significantly less than the other two methods, signaling a severe underestimation of the form that plagues the original Hirshfeld-atom.[23] It is thought that the LiC_6 graphite intercalation compound undergoes a near unity transfer of the single Li valence electron, which equates to a −0.167 e/C-atom charge.[12,29,30] In the present Li_2C_{12} model (Figure 1), the effective

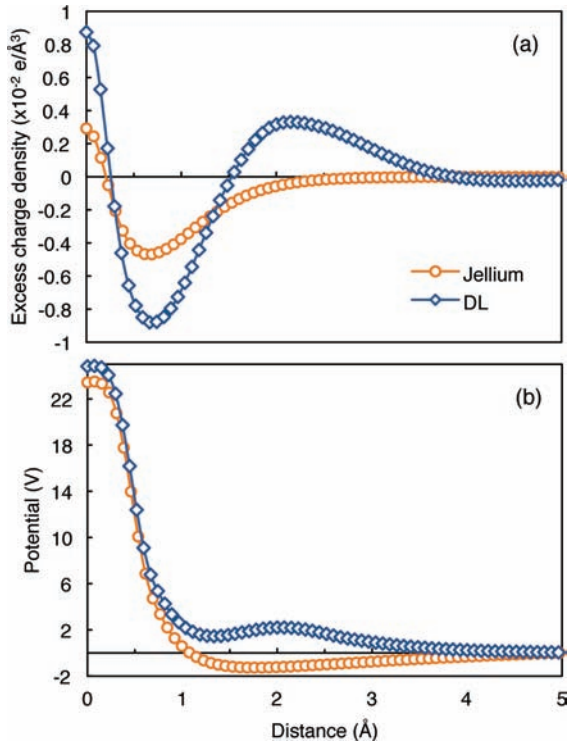

Figure 3. Comparison between the DL and jellium excess charge densities (a) and electrostatic potentials (b) as a function of the distance from the graphene layer along the direction normal to the layer. The graphene−DL ion spacing is 2 Å.

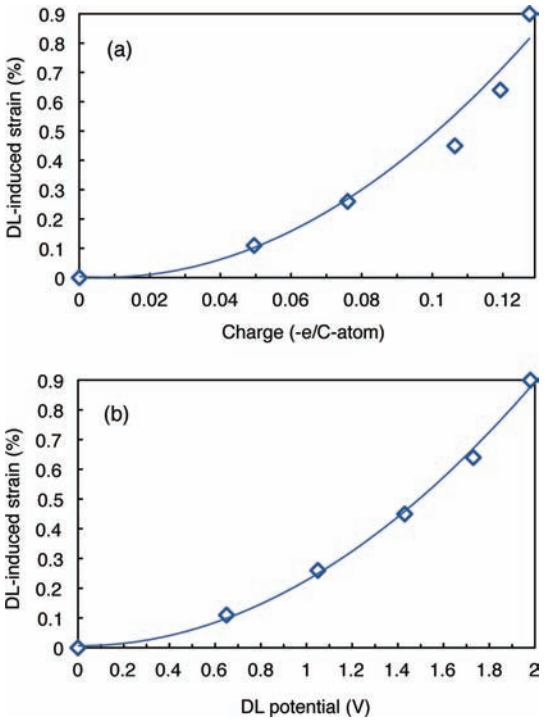

Figure 4. The DL-induced strain is the difference between the Bader-DL and jellium strains in Figure 2, shown as a function of (a) charge injection, and (b) DL potential.

cell reduces to LiC_6. Given that the calculated Bader charge is −0.11 e/C-atom (see also Figure S3, Supporting Information), at a graphene−Li ion spacing similar to that of graphite intercalation (1.85 Å), the Bader method produces results that are more commensurate with previous experimental findings.[30] Possible reasons for the discrepancy between the Bader and DDEC methods are many;[23] however, such a discussion is beyond the scope of this article.

Until now, the strains predicted via the DL model have included those due to both the quantum-mechanical (same as that of the jellium model) and electrostatic DL effects, with each effect providing some relative contribution. To verify the origin of the high strains predicted by the DL calculations, the excess charge density and electrostatic potential as a function of the distance from the graphene layer were plotted for the DL and jellium models (Figure 3). The excess charge density was generated by subtracting the first principle charge densities of the DL-charged system from that of an identical but neutral system, effectively canceling out the atomically bound core charges. At this point, it is useful to discuss the key features in Figure 3. Specifically, Figure 3a shows two excess charge polarity transitions, at distances of 0.25 and 1.3 Å. The first of these is due to the "pulling" of the graphene electrons toward the positively charged DL, leaving a region of excess positive charge near the C-atoms.[17] Hence, this crossover point is associated with the behavior of the graphene electrons, and not that of the DL ions/electrons. With this explained, and the knowledge that the graphene carries an excess negative charge while the DL ions are net positive, it is intuitive that the second transitional point describes the graphene−DL interface. This point lies between the plane of closest DL-ion approach (the so-called *outer* Helmholtz plane) and the graphene layer, so is thus within the Helmholtz (compact) layer.[33] Additionally, by tracing this point down to Figure 3b, this notion is also supported by the point of zero-gradient on the DL potential curve. In light of this, the electrostatic potential at this point can be used to describe the capacitance on the solution side,[17,33] and thus to characterize the strength of the DL.

By taking the difference between the DL and jellium strains, it is possible to determine the strain due solely to the DL presence (the DL-induced strain), and to plot these results against the injected charge (Figure 4a) and the characteristic DL potential (Figure 4b). Evidently, the charge−strain and potential−strain relationships are parabolic, with a steep ascent toward strains in excess of 1%. This observed parabolic relationship has also been seen by others experimentally.[1,34] Via inspection of Figure 3b, it is evident that the electrostatic potential in the region adjacent to the graphene layer's electronic spillover is greater for the DL model than the jellium model. In practice, higher charging of the metal electrode leads to higher electrostatic DL potentials, which occurs for the present model as the DL ions are moved closer to the graphene layer. Hence, the very high strains observed for the DL model in Figure 2 are due to the presence of the DL, the strength of which is characterized as shown in Figure 4, with DL-induced strains of 0.9% being predicted for a 2 V DL potential. To draw some comparison, in the case of chemically treated multilayer graphene sheets, actuation strains of 0.2% were shown for a 1.2 V potential.[11] In the present study, similar DL potentials result in monolayer graphene strains on the order of 0.2−0.4%, indicating a qualitative agreement with the closest available experimental results. Higher strains for monolayer graphene are intuitive in the sense that the gravimetric surface area is significantly greater (as much as five times),[1] practically resulting

in improved electrolyte access to the graphene electrode and thus greater DL formation.

In practice, one expects that macroscopic multilayer graphene sheets will be more useful given their significantly easier synthesis and higher structural rigidity. Given that the electrostatic DL effect is extremely significant (even dominant at high graphene charges) in electrochemical actuators, it will be important to maximize the electrolyte-accessible (gravimetric) surface areas of such materials in order to optimize the producible strains. Additionally, the use of IL electrolytes in such actuators should provide greater actuation performance upon fabrication. As molten salts and RTILs are similar in key features, such as their high electrode voltage accommodations (up to 5 V) and high electrolyte concentrations, we expect that our results can be used to predict the performance of RTIL-based actuators.[19] This is especially supported by the qualitative agreement between our predictions and those based on aqueous electrolyte experimental results.[1] On the basis of our calculations, although the type of ion comprising the DL is not of critical importance (see Supporting Information, Figure S4) in order to optimize the electrochemical actuation, the relative performance of Na and K DL ions is slightly better than the others tested.

CONCLUSIONS

The electrochemical actuation of monolayer graphene upon charge injection and IL electrolyte immersion was studied using ab initio DFT simulations. The computational model represented the electrostatic DL that forms aside charged surfaces in the presence of an IL electrolyte, including both the ionic and electronic interactions that exist in reality. By charging the graphene both with and without the IL electrolyte present, the precise contribution made by the DL to the overall actuation was successfully determined. Three methods of apportioning the electronic charge between the ions of the unit cell were extensively tested: the Bader, DDEC, and Hirshfeld-I methods. Of these, the Bader method was shown to produce graphene charges that are commensurate with those expected from theory and experiments. The DDEC method also yielded relatively good results, while the Hirshfeld-I scheme severely underestimated the graphene charges.

Even for moderate graphene charge injection, the contribution of the electrostatic DL to the overall strain equaled or exceeded that of the quantum-mechanical strain resulting from charge injection only. Additionally, the presence of the IL DL enabled the monolayer graphene to achieve strains in excess of one percent, which was shown to not be otherwise possible via the quantum-mechanical effect alone. This result may explain the origin of the very high electrochemical strains observed (>0.2%) and predicted (~1%) by others previously for low voltages (<3 V).[1,2] From first principle calculations, this work proves that the electrochemical actuation of covalent carbon materials, such as graphene and carbon nanotubes, in the presence of an electrolyte is predominantly due to the existence of an electrostatic DL. To optimize the actuation performance of such materials, it will be imperative to maximize the electrolyte-accessible surface areas to enhance the DL effect, and the use of IL electrolytes in order to reach maximum DL charge concentrations should prove ideal.

ASSOCIATED CONTENT

Supporting Information. Coordinates of all atoms comprising the unit cell, a figure showing the strain convergence as a function of the graphene interlayer spacing, a figure showing the resulting graphene charge injection and DL potential as a function of the graphene-DL ion spacing, and a figure showing the charge-strain response of monolayer graphene for various DL ions. This material is available free of charge via the Internet at http://pubs.acs.org.

AUTHOR INFORMATION

Corresponding Author
geoff.rogers@monash.edu; zhe.liu@monash.edu

ACKNOWLEDGMENT

The authors thank Monash University and the Victorian Partnership for Advanced Computing for their support of this research. This work was also supported by an award under the Merit Allocation Scheme on the NCI National Facility at the Australian National University. Technical assistance provided by Georg Kresse is greatly appreciated.

REFERENCES

(1) Baughman, R.; Cui, C.; Zakhidov, A.; Iqbal, Z.; Barisci, J.; Spinks, G.; Wallace, G.; Mazzoldi, A.; DeRossi, D.; Rinzler, A.; Jaschinski, O.; Roth, S.; Kertesz, M. *Science* **1999**, *284*, 1340.
(2) Madden, J.; Barisci, J.; Anquetil, P.; Spinks, G.; Wallace, G.; Baughman, R.; Hunter, I. *Adv. Mater.* **2006**, *18*, 870.
(3) Hughes, M.; Spinks, G. *Adv. Mater.* **2005**, *17*, 443.
(4) Barisci, J.; Wallace, G.; MacFarlane, D.; Baughman, R. *Electrochem. Commun.* **2004**, *6*, 22.
(5) Novoselov, K.; Geim, A.; Morozov, S.; Jiang, D.; Zhang, Y.; Dubonos, S.; Grigorieva, I.; Firsov, A. *Science* **2004**, *306*, 666.
(6) Geim, A.; Novoselov, K. *Nat. Mater.* **2007**, *6*, 183.
(7) Castro Neto, A.; Guinea, F.; Peres, N.; Novoselov, K.; Geim, A. *Rev. Mod. Phys.* **2009**, *81*, 109.
(8) Geim, A. *Science* **2009**, *324*, 1530.
(9) Bunch, J.; van der Zande, A.; Verbridge, S.; Frank, I.; Tanenbaum, D.; Parpia, J.; Craighead, H.; McEuen, P. *Science* **2007**, *315*, 490.
(10) Park, S.; An, J.; Suk, J.; Ruoff, R. *Small* **2010**, *6*, 210.
(11) Xie, X.; Qu, L.; Zhou, C.; Li, Y.; Zhu, J.; Bai, H.; Shi, G.; Dai, L. *ACS Nano* **2010**, *4*, 6050.
(12) Sun, G.; Kürti, J.; Kertesz, M.; Baughman, R. *J. Am. Chem. Soc.* **2002**, *124*, 15076.
(13) Sun, G.; Kertesz, M.; Kürti, J.; Baughman, R. *Phys. Rev. B* **2003**, *68*, 125411.
(14) Verissimo-Alves, M.; Koiller, B.; Chacham, H.; Capaz, R. *Phys. Rev. B* **2003**, *67*, 161401.
(15) Pastewka, L.; Koskinen, P.; Elsässer, C.; Moseler, M. *Phys. Rev. B* **2009**, *80*, 155428.
(16) Boda, D.; Henderson, D.; Chan, K. *J. Chem. Phys.* **1999**, *110*, 5346.
(17) Schmickler, W. *Chem. Rev.* **1996**, *96*, 3177.
(18) Armand, M.; Endres, F.; MacFarlance, D.; Ohno, H.; Scrosati, B. *Nat. Mater.* **2009**, *8*, 621.
(19) Kornyshev, A. *J. Phys. Chem. B* **2007**, *111*, 5545.
(20) Galiński, M.; Lewandowski, A.; Stępniak, I. *Electrochim. Acta* **2006**, *51*, 5567.
(21) Kresse, G.; Furthmüller, J. *Phys. Rev. B* **1996**, *54*, 169.
(22) Kresse, G.; Joubert, D. *Phys. Rev. B* **1999**, *59*, 1758.
(23) Manz, T.; Sholl, D. *J. Chem. Theory Comput.* **2010**, *6*, 2455.
(24) Charge apportionment methods other than these four were investigated also, but were found to be significantly less reliable.
(25) Tang, W.; Sanville, E.; Henkelman, G. *J. Phys.: Condens. Matter* **2009**, *21*, 084204.
(26) Bultinck, P.; Van Alsenoy, C.; Ayers, P.; Carbó-Dorca, R. *J. Chem. Phys.* **2007**, *126*, 144111.

(27) Hirshfeld, F. *Theor. Chim. Acta* **1977**, *44*, 129.
(28) Lillestolen, T.; Wheatley, R. *J. Chem. Phys.* **2009**, *131*, 144101.
(29) There remains debate as to the true charge transfers in graphite intercalation compounds. We adopt those values that have been used most recently in other actuation studies.
(30) Preil, M.; Fischer, J.; DiCenzo, S.; Wertheim, G. *Phys. Rev. B* **1984**, *30*, 3536.
(31) Fischer, J.; Kim, H.; Cajipe, V. *Phys. Rev. B* **1987**, *36*, 4449.
(32) Riemenschneider, J.; Opitz, S.; Sinapius, N.; Monner, H. *J. Intell. Mater. Syst. Struct.* **2009**, *20*, 245.
(33) Sato, N. *Electrochemistry at Metal and Semiconductor Electrodes*; Elsevier: Amsterdam, 1998; p 119.
(34) Suppiger, D.; Busato, S.; Ermanni, P. *Carbon* **2008**, *46*, 1085.